Rheological Behavior of a New Amorphous Alloy $(Al_{74}Cu_{16}Mg_{10})_{99.7}Zr_{0.3}$

Vanya DYAKOVA [1] *, Georgi STEFANOV [1], Nikolay MARINKOV [2], Stoyko GYUROV [1], Yoanna KOSTOVA [1]

[1] *Institute of Metal Science, Equipment and Technology with Hydro-and Aerodynamics Centre "Acad. A. Balevski" at Bulgarian Academy of Sciences, 67 Shipchenski Prohod Street, 1574 Sofia, Bulgaria*
[2] *Institute of General and Inorganic Chemistry at Bulgarian Academy of Sciences, Bl. 11 Acad. Angel Bonchev, 1113 Sofia, Bulgaria*

A new amorphous alloy $(Al_{74}Cu_{16}Mg_{10})_{99.7}Zr_{0.3}$ was prepared the applying a melt-spinning technique. Temperature dependence of viscosity of the alloy was determined using data from a PerkinElmer TMS2 thermo-mechanical analyzer processed according to a methodology based on the Free Volume Model (FVM). The strength of the alloy was calculated according to the Yang equation and the glass-forming ability was calculated according to the values of the Angell index m_A. The activation energy of crystallization and the activation energy of the glass transition were computed using data from differential scanning calorimetry and thermomechanical experiments respectively. The activation energy of crystallization $E_x = 168 \pm 3.7$ kJ/mol, was found to be higher than the activation energy of the glass transition $E_g = 156 \pm 1.4$ kJ/mol, which means a dominant contribution of the atomic transport barrier, compared to the nucleation barrier. The relatively high temperature interval of the supercooled melt state T_x-$T_g = 32$ K and the low viscosity values in the same range $\eta_{(Tg)} = 3.40E + 11$ Pa.s and $\eta_{(Tx)} = 1.87E + 10$ Pa.s would allow thermomechanical treatment of the alloy in the temperature range of supercooled melt.
Keywords: amorphous alloy, viscosity, free volume model, activation energy, crystallization, glass transition.

1. INTRODUCTION

The knowledge of deformation and plastic flow of materials under stress includes the elastic, viscous and plastic behaviour of bodies [1, 2]. Viscosity is the parameter, which is of special importance for the workability of amorphous alloys [3]. The temperature dependence of viscosity together with stress or strain rate effects in the supercooled liquid range, below the crystallization temperature, allows determining a processing range in which it is possible to shape these, otherwise brittle materials, into simple or more complex geometries [4]. That is why the temperature dependence of the viscosity of metallic glasses has been the subject of continuous investigations [5 – 7].

Amorphous aluminium alloys have advantages in a direct comparison of strength values with their crystal analogues [8 – 12]. These advantages become more significant when relative density is considered as the basis for strength comparison [13 – 16].

The synthesis of amorphous alloys based on aluminium is traditionally based on multicomponent systems containing aluminium (80 – 92 at.%), rare earth metals (3 – 20 at.%), transition metals (1 – 15 at.%), etc. [17]. A serious limit for the application of alloys of these systems is the high price of the components. Alloys containing widespread metals at an affordable price would have greater potential for practical application. This is the case with the ternary eutectic alloy AlCuMg which has been successfully amorphized in previous experiments [18].

The addition of a minority quantity of zirconium to the ternary eutectic alloy is expected to further enhance its ability to form glass [19, 20]. No data on the rheological behaviour of alloys with Zr concentrations below 1 at.% can be found in the literature. The aim of this research is to obtain original data on the viscosity, thermal resistance, glass forming capacity and mechanical properties of a new amorphous alloy $(Al_{74}Cu_{16}Mg_{10})_{99.7}Zr_{0.3}$.

2. MATERIALS AND METHODS

2.1. Materials

The synthesis of $(Al_{74}Cu_{16}Mg_{10})_{99.7}Zr_{0.3}$ alloy was performed in a resistance electric furnace mounted in a water-cooled pneumatic-vacuum chamber. The heating was made in an argon environment of 99.998 % purity. The resulting ingot was placed in a quartz nozzle and melted in an inductor at a temperature of 535 °C to 540 °C. This temperature exceeded approximately by 30 – 35 °C the melting temperature of the eutectic alloy E5 from the ternary equilibrium diagram of Al-Cu-Mg [21]. The temperature was controlled with a laser pyrometer of an accuracy of 0.5 °C. The amorphous state of $(Al_{74}Cu_{16}Mg_{10})_{99.7}Zr_{0.3}$ alloy was produced by rapid quenching of the melt by applying a melt-spinning technique. The surface velocity of the copper quenching disc with a diameter of 140 mm was in the range of 2900 – 3000 rpm.

---

* Corresponding author. Tel.: +359-02-4626360; fax: +359-02-46262202.
E-mail address: *v_diakova@ims.bas.bg* (V. Dyakova)

2.2. Experimental methods

The chemical composition of the obtained rapidly solidified ribbon $(Al_{74}Cu_{16}Mg_{10})_{99.7}Zr_{0.3}$ was determined by energy-dispersive X-ray spectroscopy (EDXS) on a HIROX 5500 scanning electron microscope (SEM) with a BRUCKER EDS system. The amorphousness of the ribbon was proven by X-ray powder diffraction (XRD) with a Bruker D8 Advance powder X-ray diffractometer with CuKα radiation (Ni filter) and LynxEye recording in a solid-state position-sensitive detector. The amorphous state was confirmed by transmission electron microscopy (TEM) using a transmission electron microscope JEOL 1011 at an accelerating voltage of 100 kV.

Differential scanning calorimetry (DSC) was performed on an STA 449 F3 Jupiter calorimeter connected to a QMS 403 AëolosQuadro mass spectrometer in an Ar environment.

The temperature dependence of the viscosity was determined from the data of the PerkinElmer TMS2 thermo-mechanical analyzer at heating rates of 5, 10 and 20 K/min according to the methodology developed by Russew and Stojanova [22, 23]. The crystallization temperature T_x, the glass transition temperature T_g and the glass-forming ability according to the values of the Angell index [24]:

$$m_A = 0.434 \left[\frac{BT_g}{(T_g - T_o)^2} + \frac{Q_\eta}{RT_g} - 1 \right], \tag{1}$$

were calculated in the concept of the Free Volume Model (FVM) [22, 23, 25]; where: T_0 is the temperature at which measurable relaxation phenomena starts; Q_η is the activation energy for the viscous flow; R is the universal gas constant. The strength of $(Al_{74}Cu_{16}Mg_{10})_{99.7}Zr_{0.3}$ amorphous alloy was determined according to Yang [26] equation:

$$\sigma_f = 55 \frac{\Delta T_g}{V_m}, \tag{2}$$

where σ_f is fracture strength; ΔT_g is the difference between glass transition temperature T_g and room temperature, V_m is the molar volume of the alloy.

3. RESULTS AND DISCUSSION

The amorphous structure of the rapidly solidified ribbon $(Al_{74}Cu_{16}Mg_{10})_{99.7}Zr_{0.3}$ was proven by XRD and TEM analyses. Fig. 1 presents the XRD spectrum and TEM image of the microstructure with attached diffractogram. The absence of diffraction peaks on the XRD spectrum and of diffraction, reflexes over the diffuse diffraction ring on the TEM diffractogram are the evidence for the amorphous nature of the samples.

The temperature dependence of the alloy viscosity in a region close to the glass transition temperature was calculated from the data of thermomechanical analysis, processed according to a methodology based on the FVM [22, 23].

The deformation of amorphous ribbons $\Delta = l_0 - l_T$ obtained from data of thermo-mechanical analysis (TMA) at a heating rate of 5 K/min, and a load of 70 g and 120 g

are presented in Fig. 2. The higher the temperature, the lower the viscosity of the metallic glass and, accordingly, the greater the deformation. The deformation reaches maximum values at the beginning of crystallization and breakage.
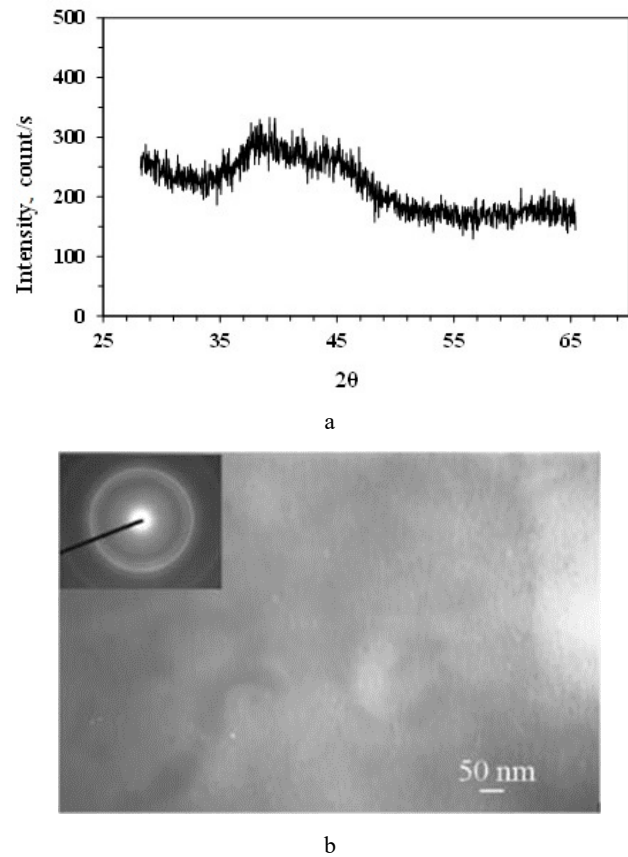

a

b

Fig. 1. Amorphous $(Al_{74}Cu_{16}Mg_{10})_{99.7}Zr_{0.3}$ ribbon: a – XRD spectrum; b – TEM image of the microstructure
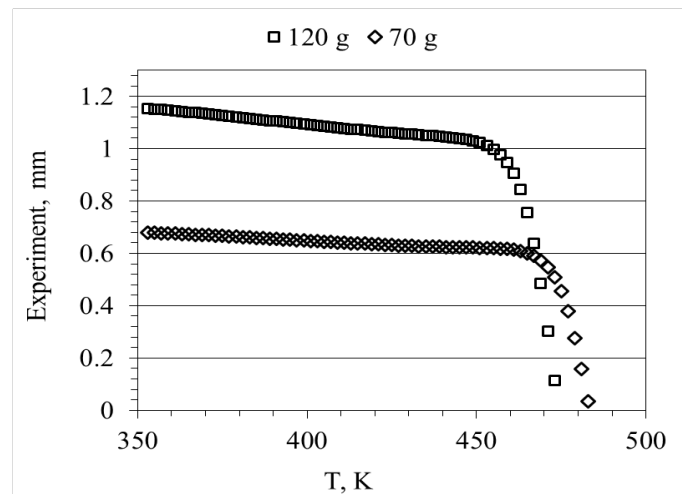

Fig. 2. Experimental TMA deformation curves at a heating rate of 5 K/min, and a load of 50 g and 70 g

The elongation curves of the ribbons $(l_0 - l_T)$ at a heating rate of 5 K/min, and loads of 70 g and 120 g are presented in Fig. 3. In the low temperature range (up to approximately 350 K), both curves practically coincide. In the high temperature range, an expressed influence of the load is demonstrated. This is because of the particularly substantial

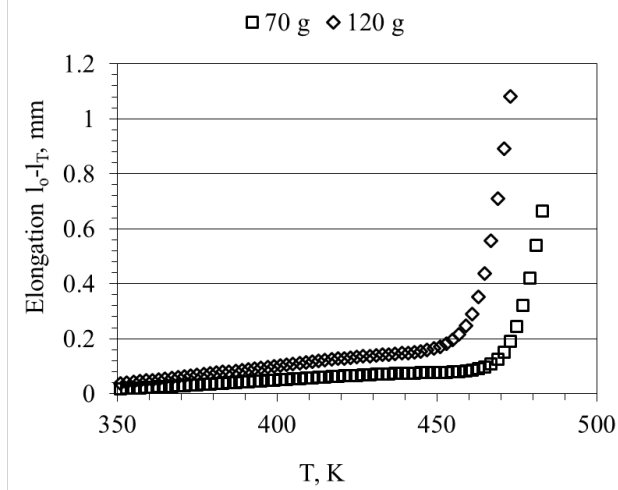contribution of viscous flow to the overall elongation (deformation).

Fig. 3. Elongation curves of the ribbons (l_0-l_T) at a heating rate of 5 K/min, and loads of 70 g and 120 g

The total deformation $\varepsilon(T)$ of an amorphous ribbon under an applied normal stress σ, at temperature T, during continuous heating, can be represented as follows [22]:

$$\varepsilon(T)=\left[l(T)-l_0\right]/l_0 = \varepsilon_\sigma^{el}(T)+\varepsilon_\sigma^{an}(T)+\varepsilon_\sigma^{rel}(T)+\varepsilon_\sigma^{te}(T)+\varepsilon_\sigma^{yf}(T) \quad (3)$$

where l_0 is the initial length, $l_{(T)}$ is the length of the sample at temperature T; $\varepsilon_\sigma^{el}(T)=\sigma/E(T)$ is the elastic strain of the ribbon at the Young's elasticity modulus of the material $E_{(T)}$; $\varepsilon_\sigma^{an}(T)$ represents the possible contribution of deformation caused by an elasticity; $\varepsilon_\sigma^{rel}(T)$ shows the contribution of relaxation effects to the overall strain; $\varepsilon_\sigma^{te}(T)$ represents the contribution of the thermal expansion of both the specimen and the grips and $\varepsilon_\sigma^{yf}(T)$ shows the contribution of the viscous flow to the overall strain.

It was shown in [22] that the subtraction of the strains obtained at different loads gives:

$$\Delta\varepsilon_{1,2}(T)= \varepsilon_{\sigma_1}(T)-\varepsilon_{\sigma_2}(T)\cong \varepsilon_{\sigma_1}^{yf}(T)-\varepsilon_{\sigma_2}^{yf}(T), \quad (4)$$

where $\Delta\varepsilon_{1,2}(T)$ is caused by the effective stress $\Delta\sigma_{1,2}=\sigma_1-\sigma_2$. Applying the Newtonian relation for viscous flow $\eta=\tau/\dot\varepsilon$ and taking into account that the shear stress $\tau=\sigma/3$ we obtain

$$\Delta\dot\varepsilon_{1,2}(T)=\frac{\Delta\tau_{1,2}}{\eta(T)}, \quad (5)$$

where $\Delta\dot\varepsilon_{1,2}(T)=\dot\varepsilon_1(T)-\dot\varepsilon_2(T)$ is difference between strain rates $\dot\varepsilon_1$ and $\dot\varepsilon_2$, caused by applied shear stresses τ_1 and τ_2, and $\Delta\tau_{1,2}=\tau_1-\tau_2$.

The determination of the temperature dependence of the viscosity close to the glass transition temperature can be traced in detail using the experimental results. A typical temperature dependence of the strain rate $\Delta\dot\varepsilon(T)$ induced by shear stresses $\Delta\tau_{1-2}=1/3(\sigma_1-\sigma_2)$ for the case $\sigma_1=120$ g, $\sigma_2=70$ g is shown in Fig. 4.
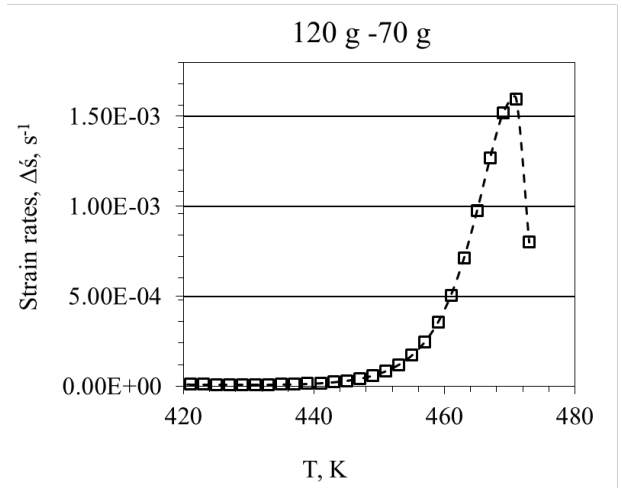

Fig. 4. Temperature dependence of the strain rates obtained at load difference (120 g – 70 g)

The curve in Fig. 4 was obtained by numerical differentiation of the temperature dependence of the degree of deformation (l_0-l_T). The strain rate remains unchanged up to temperature of 435 K. Above this temperature, a rapid increase of the strain rate is observed resulting on passing through glass transition temperature T_g. The transition of the strain rate through a maximum shows that the temperature of the beginning of primary crystallization T_{on} is reached.

The temperature dependence of the viscosity, calculated from the experimental data for the strain rate values is presented on Fig. 5. The points show the experimental data, the solid line is the least squares' fit over all experimental data.
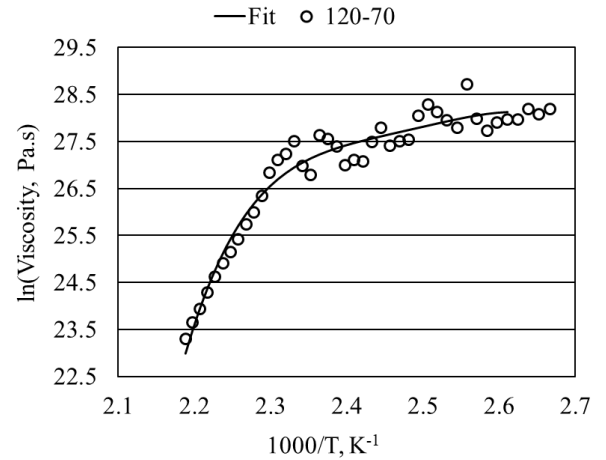

Fig. 5. Temperature dependence of viscosity of $(Al_{74}Cu_{16}Mg_{10})_{99.7}Zr_{0.3}$ glassy alloy at a heating rate of 5 K/min

The steep part of the curve approaches the quasi-equilibrium structural state of a supercooled metal melt. The other part of the curve, in the region of low temperatures, is the non-equilibrium viscosity of the vitrified alloy.

Fig. 6 shows the measured (bubble line) and calculated according to the FVM (solid line) temperature dependences of the viscosity of the amorphous alloy at a heating rate of 5 K/min [22, 23]. The dashed line is the temperature dependence of the quasi-equilibrium viscosity η_{eq}. The solid curve describes the fit according to the FVM.
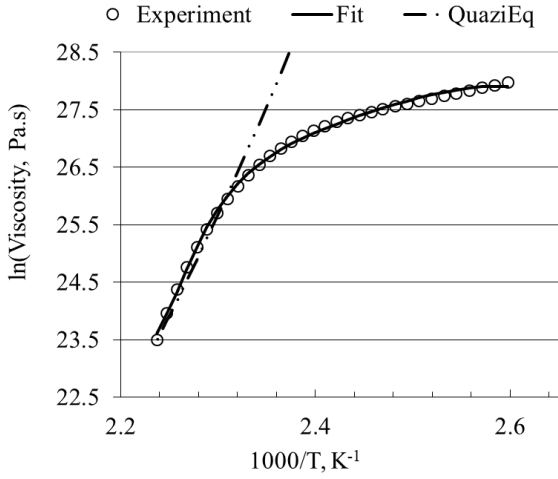
Fig. 6. Temperature dependence of viscosity according to the FVM of $(Al_{74}Cu_{16}Mg_{10})_{99.7}Zr_{0.3}$ glassy alloy at a heating rate of 5 K/min

Fig. 7. Temperature dependence of the viscosity of $(Al_{74}Cu_{16}Mg_{10})_{99.7}Zr_{0.3}$ glassy alloy according to the FVM at a heating rate of 10 K/min

The intersection point of the non-equilibrium and quasi-equilibrium curves determines the glass transition temperature T_g.

The glass transition temperature T_g and the viscosity value $\eta(T_g)$ are presented in Table 1 together with the FVM model parameters, where v_r is the attempt frequency; Q_r is the activation energy for relaxation; Q_η is the activation energy for viscous flow; $c_{f,o}$ is the initial concentration of frozen-in structural (flow) defects, T_o is the temperature at which a relaxation effect is observed; B presented as $B \cong \gamma \alpha_v^{-1} v / \Omega_o$, where $\alpha_v = 3\alpha_l$ is the thermal coefficient of volume expansion, and $\gamma \Omega_o$ is the mean atomic volume at dense random packing (DRP); and η_o is the viscosity pre-exponential factor, all obtained by regression analysis of the experimental data, σ_f is fracture strength. The calculated value of the Angell fragility index $m_A = 35$ is evidence of comparatively high glass-forming ability of the studied alloy. The temperature dependences of the viscosity of $(Al_{74}Cu_{16}Mg_{10})_{99.7}Zr_{0.3}$ alloy at heating rates of 10 and 20 K/min respectively are presented on Fig. 7 and Fig. 8.

The T_g values obtained at the three applied heating rates of 5, 10 and 20 K/min were used to determine the glass transition activation energy.

It is practically impossible to determine the glass transition temperature T_g from the DSC diagrams over the entire range of heating rates due to the weak thermal effect. For this type of alloys, Janovszky et. al [27] recommend the T_g temperature to be determined by another method.
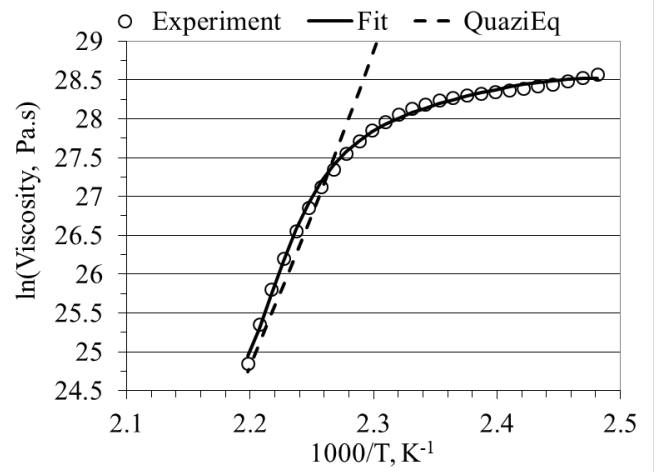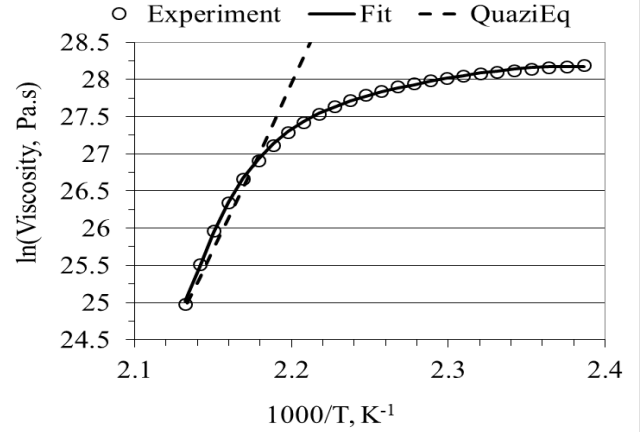

Fig. 8. Temperature dependence of the viscosity of $(Al_{74}Cu_{16}Mg_{10})_{99.7}Zr_{0.3}$ glassy alloy according to the FVM at a heating rate of 20 K/min

We used the data from the DSC experiment (Fig. 9) to calculate the activation energy of crystallization, while the activation energy of the glass transition was computed using data from the thermomechanical experiment. The activation energies were calculated according to the Kissinger method [28, 29] using the values of the crystallization peak and the glass transition temperature at different heating rates (Fig. 10 and Fig. 11).
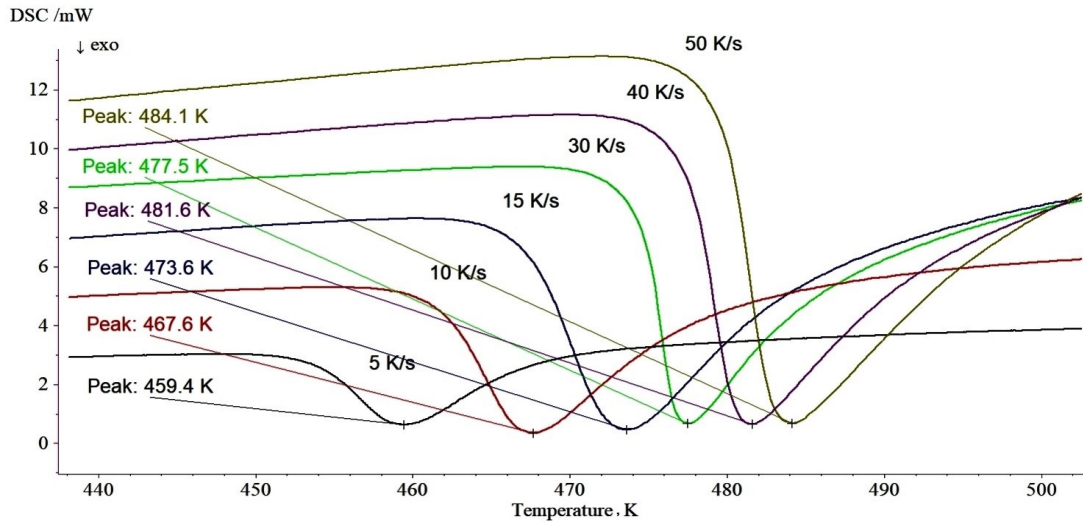
Table 1. The glass transition temperature T_g, the viscosity value $\eta_{(Tg)}$ and the FVM model parameters

Parameter	Value	Dimension	Parameter	Value	Dimension
v_r	2.81E+09	1/s	B	1720.493	K
Q_r	36.8266	kJ/mol	η_o	1.38E-11	Pa.s/K
$c_{f,o}$	2.5E-06		m_{Angel}	35	
R	8.31451	J/mol.K	T_g	427	K
T_o	308	K	$\eta(T_g)$	3.40E+11	Pa.s
dT	0.25	K	$\eta(T_x)$	1,87E+10	Pa.s
Q_η	108.4337	kJ/mol	σ_f	793	MPa

Fig. 9. DSC diagrams of $(Al_{74}Cu_{16}Mg_{10})_{99.7}Zr_{0.3}$ glassy ribbon, obtained at heating rates in the range 5 – 50 K/min
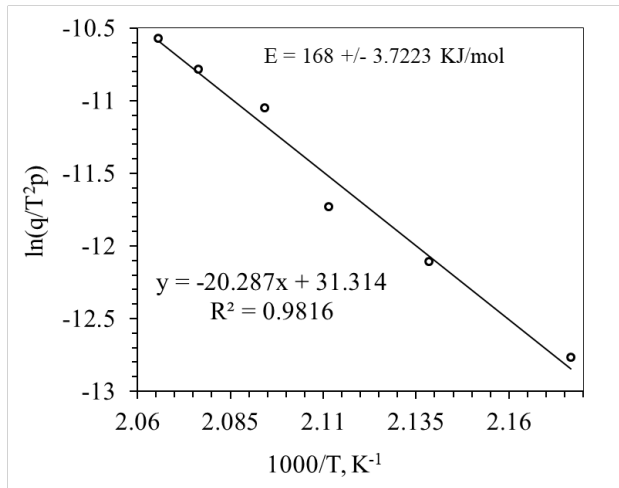

Fig. 10. Kissinger plot of temperature of crystallization T_{max} (temperature of the maximum of the first crystallization peak)
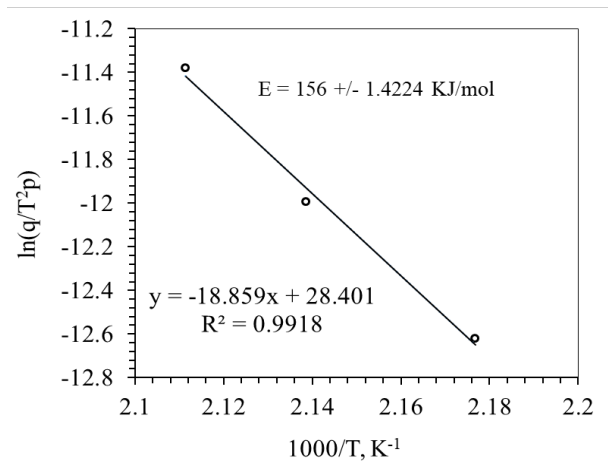

Fig. 11. Kissinger plot of glass transition temperature T_g

The activation energy of the glass transition can be considered as an energy barrier for mass transport, which is usually evaluated from the temperature dependence of the viscosity. Both activation energies (of viscous flow and glass transition) reflect the transition from a solid glassy state to a supercooled melt, i.e. unlocking of cooperative atomic mobility [30]. The activation energy of crystallization of the studied $(Al_{74}Cu_{16}Mg_{10})_{99.7}Zr_{0.3}$ glassy alloy $E_x = 168 \pm 3.7$ kJ/mol (Fig. 11), is higher than the activation energy of the glass transition $E_g = 156 \pm 1.4$ kJ/mol (Fig. 10), which shows the dominant contribution of the atomic transport barrier, compared to the nucleation barrier, in the total crystallization energy barrier of the supercooled melt.

4. CONCLUSIONS

Original data were obtained on the temperature dependence of the viscosity in the glass transition region of an $(Al_{74}Cu_{16}Mg_{10})_{99.7}Zr_{0.3}$ alloy.

The glass-forming ability of the alloy was obtained according to the values of the Angell index m_{Angel} and the strength of the alloy was calculated according to the Yang equation.

The comparison of crystallization and glass transition activation energy values gives us reason to claim that the atomic transport barrier has a dominant role in the overall crystallization energy barrier.

The relatively high temperature interval of the supercooled melt T_x-$T_g = 32$ K and the low viscosity values in the same range $\eta(T_g) = 3.40E + 11$Pa.s and $\eta(T_x) = 1.87E + 10$Pa.s would allow thermomechanical treatment of $(Al_{74}Cu_{16}Mg_{10})_{99.7}Zr_{0.3}$ alloy in the temperature range of supercooled melt.

Acknowledgments

REFERENCES

1. **Wilson, D.** What is Rheology? *Eye* 32 (2) 2018: pp. 179 – 183.
    https://doi.org/10.1038/eye.2017.267

2. **Faith, A.** Understanding Rheology. Oxford University Press, 2001: pp. 560.
    https://global.oup.com/ushe/product/understanding-rheology-9780195141665?cc=bg&lang=en&

3. **Keryvina, V., Gueguena, Y., Bernard, C.** Assessment of Rheological and Thermodynamic Properties of the Pd40Ni40P20 Bulk Metallic Glass around Glass Transition Using an Indentation Creep Technique *Journal of Alloys and Compounds* 509 (1) 2011: pp. S18 – S22.
https://doi.org/10.1016/j.jallcom.2010.12.11

4. **Schroers, J., Hodges, T.M., Kumar, G., Raman, H., Barnes, A.J., Pham, Q., Waniuk, T.A.** Thermoplastic Blow Molding of Metals *Materials Today* 14 (1 – 2) 2011: pp. 14 – 19.
https://doi.org/10.1016/S1369-7021(11)70018-9

5. **Schroers, J.** The Superplastic Forming of Bulk Metallic Glasses *The Journal of The Minerals, Metals & Materials Society* 57 2005: pp. 35 – 39.
https://doi.org/10.1007/s11837-005-0093-2

6. **Schroers, J.** On the Formability of Bulk Metallic Glass in its Supercooled Liquid State *Acta Materialia* 56 (3) 2008: pp 471 – 478.
https://doi.org/10.1016/j.actamat.2007.10.008

7. **Mukherjee, S., Schroers, J., Zhou, Z., Johnson, W.L., Rhim, W.K.** Viscosity and Specific Volume of Bulk Metallic Glass-Forming Alloys and their Correlation with Glass Forming Ability *Acta Materialia* 52 (12) 2004: pp. 3689 – 3695.
https://doi.org/10.1016/j.actamat.2004.04.023

8. **Zhang, W., Wang, W.H., Greer, A.L.** Processing and Properties of Metallic Glass *Progress in Materials Science* 83 2016: pp. 152 – 283.

9. **Schuh, C.A., Hufnagel, T.C., Ramamurty, U.** Mechanical Behavior of Amorphous Alloys *Acta Materialia* 55 (12) 2007: pp. 4057 – 4109.
https://doi.org/10.1016/j.actamat.2007.01.052

10. **He, Y., Poon, S.J., Shiflrt, G.J.** Synthesis and Properties of Metallic Glasses That Contain Aluminum *Science* 241 1988: pp. 1640 – 1642.
https://www.science.org/doi/10.1126/science.241.4873.1640

11. **Greer, A.L., Cooper, P.S., Meredith, M.W., Schneider, W., Schumacher, P., Spittle, J.A., Tronche, A.** Grain Refinement of Aluminium Alloys by Inoculation *Advanced Engineering Materials* 5 (1 – 2) 2003: pp. 81 – 91.
https://doi.org/10.1002/adem.200390013

12. **Inoue, A.** Amorphous, Nanoquasicrystalline and Nanocrystalline Alloys in Al-based Systems *Progress in Materials Science* 43 (5) 1998: pp. 365 – 520.
https://www.sciencedirect.com/journal/progress-in-materials-science/vol/43

13. **Inoue, A.** High-Strength Bulk Amorphous-Alloys with Low Critical Cooling Rates *Materials Transactions JIM* 36 (7) 1995: pp. 866 – 875.
http://dx.doi.org/10.2320/matertrans1989.36.866

14. **Greer, A.L.** Partially or Fully Devitrified Alloys for Mechanical Properties *Materials Science and Engineering: A* 304 – 306 2001:pp. 68 – 72.
https://doi.org/10.1016/S0921-5093(00)01449-0

15. **Shiflet, G.J., He, Y., Poon, S.J.** Mechanical Properties of Aluminium-rich Al–Fe Gd Metallic Glass *Scripta Metallurgica* 22 (10) 1988: pp. 1661 – 1664.
https://www.osti.gov/biblio/5855828

16. **He, Y., Dougherty, G., Shiftlet, G., Poon, S.** Unique Metallic Glass Formability and Ultra-high Tensile Strength in AlNiFeGd Alloys *Acta Metallurgica et Materialia* 41 (2) 1993: pp: 337 – 343.
https://doi.org/10.1016/0956-7151(93)90064-Y

17. **Cahn, R.** Aluminium-based Glassy Alloys *Nature* 341 1989: pp. 183 – 184.
https://doi.org/10.1038/341183a0

18. **Kang, C.K., Sung, H.P., Min, Y.N., Won, T.K., Do, H.K.** Synthesis of Amorphous Matrix Nano-composite in Al-Cu-Mg Alloy *Applied Microscopy* 44 (3) 2014: pp. 105 – 109.
https://doi.org/10.9729/AM.2014.44.3.105

19. **Pilarczyk, W.** The Study of Structure and Glass Forming ability of Zr-based Amorphous Alloy *Archives of Materials Science and Enginering* 63 (1) 2013: pp. 13 – 25.

20. **Chen, N., Wang, G.** The Effect of Zr Addition on the Glass-forming Ability and Thermal Stability of Al-based Amorphous Alloys *Journal of Non-Crystalline Solids* 521 2019: pp. 119481.

21. **Ravghavan, V.** Al-Cu-Mg Diagram *Journal of Phase Equilibria and Diffusion* 28 2007: pp. 174 – 179.
https://doi.org/10.1007/s11669-007-9045-6

22. **Russew, K., Stojanova, L.** Glassy Metals, Springer-Verlag Berlin, Heidelberg, 2016.
https://doi.org/10.1007/978-3-662-47882-0

23. **Stojanova, L., Russew, K., Fazakas, E., Varga, L.K.** Thermo-mechanical Study of Rapidly Solidified Amorphous Alloys $Al_{85}Ni_5Co_2RE_8$ *Journal of Alloys and Compounds* 540 2012: pp. 192 – 197.
https://doi.org/10.1016/j.jallcom.2012.06.095

24. **Angell, C., Monnerie, L., Torell, L.** Strong and Fragile Behaviour in Liquid Polymers *MRS Online Proceedings Library* 215 1990: pp. 3 – 9.
https://doi.org/10.1557/PROC-215-3

25. **Turnbull, D.** Free-Volume Model of the Amorphous Phase: Glass Transition *Journal of Chemical. Physics* 34 1961: pp. 120.
https://doi.org/10.1063/1.1731549

26. **Yang, B.** Unified Equation for the Strength of Bulk Metallic Glasses *Applied. Physics Letters* 88 2006: pp. 221911.
https://doi.org/10.1063/1.2206099

27. **Janovszky, D., Sveda, M., Sycheva, A., Kristaly, F., Zámborszky, F., Koziel, T., Piotr, B., Gyorgy, C., Kaptay, G.** Amorphous Alloys and Diferential Scanning Calorimetry (DSC) *Journal of Thermal Analysis and Calorimetry* 147 2022: pp. 7141 – 7157.
https://doi.org/10.1007/s10973-021-11054-0

28. **Kissinger, H.E.** Variation of Peak Temperature with Heating Rate in Differential Thermal Analysis *Journal of Research of the National Bureau of Standards* 57 (4) 1956: pp. 217 – 221.
https://nvlpubs.nist.gov/nistpubs/jres/057/jresv57n4p217_a1b.pdf

29. **Kissinger, H.E.** Reaction Kinetics in Differential Thermal Analysis *Analytical Chemistry* 29 (11) 1957: pp. 1702 – 1706.
https://doi.org/10.1021/ac60131a045

30. **Chen, N., Yang, H.A., Caron, A., Chen, P.C., Lin, Y.C., Louzguine-Luzgin, D.V., Yao, K.F., Esashi, M., Inoue, A.** Glass-forming Ability and Thermoplastic Formability of a Pd40Ni40Si4P16 Glassy Alloy *Journal of Materials Science* 46 2011: pp. 2091 – 2096.
https://doi.org/10.1007/s10853-010-5043-x